http://dx.doi.org/10.5012/bkcs.2013.34.5.1383

Influence of Thiol Molecular Backbone Structure on the Formation and Reductive Desorption of Self-Assembled Aromatic and Alicyclic Thiol Monolayers on Au(111) Surface

Hungu Kang and Jaegeun Noh*

Department of Chemistry and Institute of Nano Science and Technology, Hanyang University, Seoul 133-791, Korea
**E-mail: jgnoh@hanyang.ac.kr*
Received January 22, 2013, Accepted February 7, 2013

The surface structure and electrochemical behavior of self-assembled monolayers (SAMs) prepared from benzenethiol (BT), cyclohexanethiol (CHT), and cyclopentanethiol (CPT) on Au(111) surface were examined by scanning tunneling microscopy (STM) and cyclic voltammetry (CV) to understand the influence of thiol molecular backbone structure on the formation and reductive desorption behavior of SAMs. STM imaging showed that BT and CPT SAMs on Au(111) surface formed at room temperature were mainly composed of disordered domains, whereas CHT SAMs were composed of well-ordered domains with three orientations. From these STM results, we suggest that molecule-substrate interaction is a key parameter for determining the structural order and disorder of simple aromatic and alicyclic thiol SAMs on Au(111). In addition, the reductive desorption peak potential for BT SAMs with aromatic rings was observed at a less negative potential of –566 mV compared to CHT SAMs (–779 mV) or CPT SAMs (–775 mV) with aliphatic cyclic rings. This reductive desorption behavior for BT SAMs is due to the presence of *p*-orbitals on the aromatic rings, which promote facile electron transfer from the Au electrode to BT as compared to CHT and CPT. We also confirmed that the reductive desorption behavior for simple alicyclic thiol SAMs such as CHT and CPT SAMs on Au electrodes was not significantly influenced by the degree of structural order.

Key Words : Benzenethiol, Cyclohexanethiol, Cyclopentanethiol, Self-assembled monolayers, Reductive desorption

Introduction

The spontaneous adsorption of organic thiols onto metal surfaces creates self-assembled monolayers (SAMs) that are key building blocks for tailoring the physical and chemical properties of surfaces and for fabrication of functional nanostructures.[1-5] In particular, SAMs of alkanethiols with simple aliphatic chains are considered the best model systems for understanding fundamental issues such as molecular self-assembly, two-dimensional (2D) phase transition, 2D packing structure, thermal and temporal stability, and adsorption state.[1-4,6-15] Scanning tunneling microscopy (STM) imaging with molecular-scale spatial resolution has revealed that alkanethiol SAMs at saturation coverage on Au(111) surface have a well-ordered $(\sqrt{3} \times \sqrt{3})R30^{o}$ structure or a $c(4\sqrt{3} \times 2\sqrt{3})R30^{o}$ superlattice (often denoted as a $c(4 \times 2)$ superlattice).[3,4,7-9,14] On the other hand, SAMs from aromatic thiols with p-conjugated phenyl rings have drawn much attention due to their potential use in molecular electronic applications.[15-22] It has been realized that SAM-based device performance is greatly influenced by the molecular orientation, packing structure, adsorption conditions, and structural order of the SAMs. Hence, it is very important to develop preparative methods to obtain high-quality aromatic thiol SAMs with a uniform, ordered packing structure, which could be attained by tuning experimental conditions[23,24] and backbone structure,[25,26] and by displacement techniques[27] and microwave treatment.[28] Alicyclic thiols with flexible aliphatic rings can be precursors for preparing SAMs on gold surfaces.[10,27,29-33] It was reported that SAMs derived from cyclohexanethiol (CHT) could be utilized as effective temporary layers for guiding the well-ordered two-dimensional (2D) SAM growth of benzenethiol (BT) SAMs.[27] 4-Cyclohexyl substituted CHT SAMs can be used as an excellent resist for patterning by electron irradiation.[33]

From numerous investigations, it was realized that the formation of 2D SAMs was mainly driven by the interactions both between the sulfur headgroup-gold substrate and between the molecular backbones. In particular, the packing structure, order, and stability of SAMs were significantly influenced by the chemical structure of the organic thiol molecular backbone. To understand these fundamental issues, STM has been used as one of the very powerful tools for visualizing the atomic- and molecular-scale surface structures of SAMs on metal surfaces, as demonstrated in many previous reports.[1-4,6-16,20-33] Additionally, thermal desorption spectroscopy (TDS)[10,11,32,34-37] and electrochemical measurements[38-43] are very useful techniques to investigate the adsorption conditions, thermal stability, and the electrochemical behavior and stability of SAMs. TDS measurements revealed that alkanethiol SAMs exist as a form of monomer (alkanethiolate), not dimers (dialkyl disulfides) derived from associa-

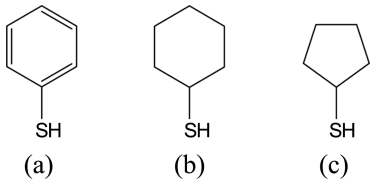

Figure 1. Chemical structures of target molecules used in this study: (a) benzenethiol (BT), (b) cyclohexanethiol (CHT), and (c) cyclopentanethiol (CPT).

tive reactions of the sulfur headgroups,[10,11,34,36] while electrochemical measurements have shown that alkanethiolates with longer alkyl chains have more negative peak potential for reductive desorption compared to those with shorter chains, implying that van der Waals interactions among alkyl chains are a crucial factor for enhancing electrochemical stability.[38-42] To date, however, there have been no reports directly comparing the formation and reductive desorption behavior of organic thiol SAMs with aromatic and alicyclic molecular backbones. Therefore, to better understand these issues, we investigated three types of molecules: BT with an aromatic ring, CHT with a six-membered aliphatic ring, and cyclopentanethiol (CPT) with a five-membered aliphatic ring (Figure 1). By comparing the results obtained from BT, CHT, and CPT SAMs, we sought to understand the effects of the π-conjugated aromatic ring and the size of the aliphatic ring on the formation and electrochemical behavior of SAMs. In this work, we clearly demonstrated that the aromatic and alicyclic molecular backbones of organic thiols significantly affect the formation and reduction desorption behavior of SAMs.

Experimental Section

BT, CHT, and CPT were purchased from Tokyo Chemical Industry (Tokyo, Japan) and were used without further purification. Au(111) substrates with atomically flat terraces of 100-300 nm in diameter were prepared by thermal evaporation of gold onto freshly cleaved mica sheets prebaked at 330 ºC under a vacuum pressure of 10^{-5}-10^{-6} Pa.[8] BT, CHT, and CPT SAMs were prepared by immersing the Au(111) substrates in freshly prepared 1 mM ethanol solutions of the corresponding thiols at room temperature for 24 h. After the SAM samples were taken from the solutions, they were thoroughly rinsed with pure ethanol to remove physisorbed molecules from the surface and were dried in a stream of nitrogen.

STM measurements (NanoScope E, Veeco, Santa Barbara, CA, USA) were performed in air with mechanically cut Pt/Ir tips (80:20). All STM images were acquired in constant current mode using a sample positive bias voltage (V_b) ranging from 400 to 500 mV and a tunneling current (I_t) ranging from 150 to 400 pA between the tip and sample. Electrochemical experiments were conducted with an electrochemical system (BAS-100) employing a three-electrode cell. Gold electrodes coated with BT, CHT, or CPT SAMs were used as the working electrodes, and platinum wire and Ag/AgCl (KCl sat.) were used as the counter and reference electrodes, respectively. For cyclic voltammograms, all solutions contained 1 mM $K_4[Fe(CN)_6]$ and 1 M KNO_3 aqueous electrolyte, and they were thoroughly deaerated by bubbling nitrogen gas through the solution for 30 min before each experiment. The system was cycled at a scan rate of 50 mV/s between −400 and +800 mV. For reductive desorption measurements, samples were immersed in an electrochemical cell filled with a solution of 0.5 M NaOH degassed for 30 min prior to use. Linear sweep voltammograms of SAM samples were recorded with a potential scan rate of 50 mV/s in the range from −400 to −1000 mV.

Results and Discussion

The STM images in Figure 2 clearly show a significant difference in the formation and surface structures of BT, CHT, and CPT SAMs on Au(111) surface formed after immersion for 24 h in 1 mM ethanol solutions of the corresponding thiols at room temperature. As revealed by several earlier studies of our group and others,[4,25-28] the adsorption of BT molecules (BTs) with π-conjugated aromatic rings on the Au(111) surface mainly formed poorly ordered SAMs with many aggregated bright domains, as shown in Figure 2(a). Figure 2(a') shows the height profile along line (a') on the STM image of Figure 2, and reveals that the bright domains have a protrusion of 0.25 nm, which is nearly the same as the monatomic step height of Au. Therefore, the bright domains are considered as Au adatom islands, and they appeared due to from the low mobility of Au adatoms that emerge from chemisorption of BTs on the Au(111)

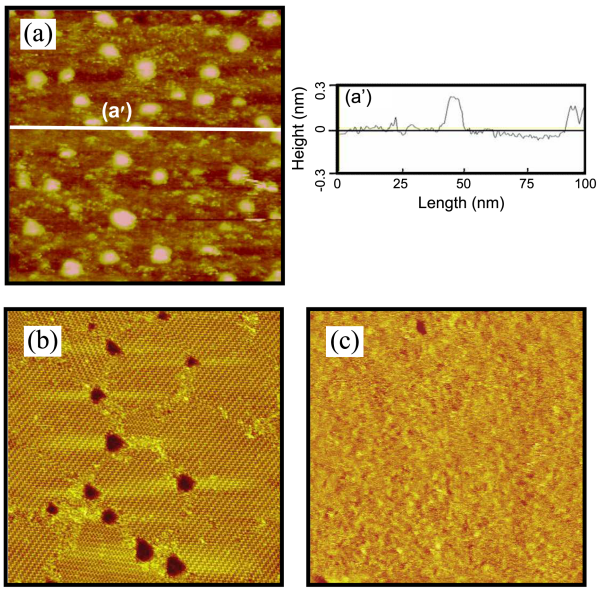

Figure 2. STM images of aromatic and alicyclic SAMs on Au(111) surfaceformed after 24 h immersion in a 1 mM ethanol solution of the thiol at room temperature: (a) BT SAMs, (b) CHT SAMs, and (c) CPT SAMs. The scan size for all STM images was 100 nm × 100 nm. Imaging parameters were (a) I_t = 0.15 nA and V_b = 500 mV, (b) I_t = 0.4 nA and V_b = 500 mV, and (c) I_t = 0.25 nA and V_b = 450 mV.

surface, as suggested by previous work.[4] In contrast to BT, the adsorption of CHT molecules (CHTs), which have aliphatic rings, led to the formation of well-ordered SAMs containing three domain orientations and boundaries, as shown in Figure 2(b). CHT SAMs also contained vacancy islands (VIs) that have been typically observed for the solid phases of closely packed and ordered alkanethiol SAMs. It is interesting to note that even though the CHT ring has various dynamic structural conformers,[30,44] CHTs always formed ordered SAMs driven by optimization of van der Waals interactions between the aliphatic rings.[29,31,45] STM and surface enhanced Raman scattering measurements suggested that CHT SAMs on Au(111) surface contained two energetically stable conformers, *i.e.*, equatorial and axial chair conformations.[29,30] Structural details from the molecular-scale viewpoint have been described previously in the literature.[29]

An interesting question is why BTs on Au(111) surface have difficulty forming ordered SAMs, unlike CHTs, as shown in Figures 2(a) and 2(b). It is well known that the molecular backbone of thiols are oriented parallel to the gold surface in the initial SAM growth stage. As a result, interactions between molecules and substrate would be maximized in this initial stage, resulting in the formation of lying down striped phases.[9] As surface coverage increases with increasing immersion time, the number of molecules with an upright geometry would increase due to phase transition from the striped phase to the upright phase. If interactions between the π-conjugated aromatic rings of BTs and the gold substrate are relatively stronger than the van der Waals interactions between BT aromatic rings, only some BTs would be able to change their adsorption geometry to the upright phase upon increased immersion time, while other BTs would remain unchanged in adsorption geometry. Near-edge X-ray absorption spectroscopy and STM measurement results suggested that the BT aromatic rings had a nearly flat lying adsorption geometry,[46] as expected. Therefore, it is reasonable to consider the formation of disordered phases in Figure 2(a) being due mainly to the presence of mixed phases with lying down and upright geometries. However, CHTs usually form well-ordered 2D SAMs, as shown in Figure 2(b). This can be attributed to the very weak interactions between the molecular backbones of CHTs and the Au(111) surface due to the conformational dynamics in the lying down phase. Therefore, well-ordered 2D SAMs formed as a result of optimizing the van der Waals interactions between aliphatic rings.

In contrast to CHTs with a six-membered ring, CPT molecules (CPTs) with a five-membered ring at room temperature formed only disordered SAMs, as shown in Figure 2(c). The observed remarkable difference in the 2D structures of CHT and CPT SAMs can be ascribed to the large difference in their ring structures: the cyclohexyl ring of CHTs has dynamic structural conformers, while the cyclopentyl ring of CPTs has torsional strain and a nonplanar envelope structure. Hence CPTs at the initial SAM growth stage experience slightly stronger interactions between the cyclopentyl rings of CPTs and the Au(111) surface compared to the interactions between the cyclohexyl rings of CHTs with their dynamic ring conversions and the Au(111) surface. However, such interactions for CPT SAMs are probably less than for BT SAMs. Therefore, fully covered CPT SAMs with upright adsorption geometry could form after a sufficient immersion time of 24 h used in this study, but the formation of disordered phases was ascribed to the lack of crystallization of 2D CPT SAMs since CPTs can form solid-phase SAMs with a $(\sqrt{3.5} \times \sqrt{5})$R25° structure *via* long-term stabilization for one month, as revealed in previous work.[47] From the STM results, we clearly found that the molecule-substrate interaction is a crucial parameter for determining the structural order and disorder of simple aromatic and alicyclic thiol SAMs on Au(111), especially in the case of SAM systems in which the surface energy gained by weak van der Waals interactions is relatively small (or nearly the same) compared to the energy gained by molecule-substrate interactions in the lying down phase.

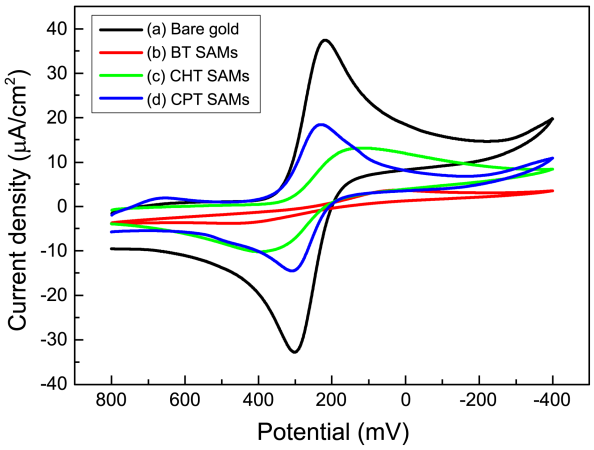

Figure 3. Cyclic voltammograms of (a) bare Au electrode, (b) BT SAM-, (C) CHT SAM-, and (d) CPT SAM-modified Au electrodes in 1 mM $K_4[Fe(CN)_6]$ containing 1 M KNO_3.

Figure 3 depicts cyclic voltammograms (CVs) of the (a) bare Au electrode, (b) BT SAM-, (c) CHT SAM-, and (d) CPT SAM-modified Au electrodes in 1 mM $K_4[Fe(CN)_6]$ containing 1 M KNO_3. The peak currents (I_p) for (a), (b), (c), and (d) were measured to be 38.85, 3.68, 13.15 and 18.39, respectively. Figure 3(a) presents a well-defined CV characteristic indicating a diffusion limited redox process of the bare Au electrode. The heterogeneous electron transfer of $Fe(CN)_6^{4-}$ ions was blocked on the Au electrodes after SAM formation, as shown in Figure 3. BT SAMs (aromatic phenyl ring) showed more effective blocking properties than CHT and CPT SAMs (alicyclic rings). This result suggests that BT SAMs formed *via* π-π stacking interactions among BTs and interactions between the aromatic ring and Au(111) surface prevent more effective electron transfer reactions between electrolytes and gold electrodes compared to CHT and CPT SAMs. On the other hand, CHT SAMs (ordered phase) have higher blocking efficiency compared to CPT SAMs (disordered phase). Therefore, the structural order for alicyclic thiol SAMs on Au(111) surface could be a major factor for blocking electron transfer reactions between the

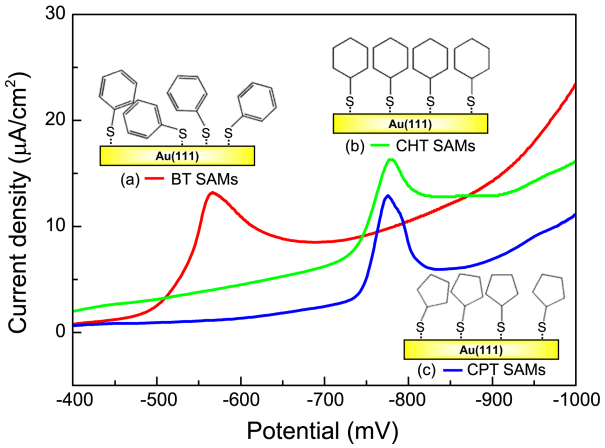

Figure 4. Reductive desorption cyclic voltammograms for (a) BT SAMs, (b) CHT SAMs, and (c) CPT SAMs on Au(111) surfacein 0.5 M NaOH.

electrolytes and gold surface.

Figure 4 shows a clear difference in reductive desorption peak potentials between aromatic thiol (BT) SAMs and alicyclic thiol (CHT and CPT) SAMs. The reductive peak potentials for (a) BT SAMs, (b) CHT SAMs, and (c) CPT SAMs on Au(111) surface in 0.5 M NaOH were observed at –566, –779, and –775 mV, respectively. In general, the reductive desorption of organic thiol SAMs occurs *via* S–Au bond cleavage when a negative potential is applied to the Au electrode. The related electrochemical half reaction is shown by the following Eq. (1).

$$R–S–Au + e^- \rightarrow R–S^- + Au \quad (1)$$

It has been reported that the reductive desorption potentials for alkanethiol or alkanedithiol SAMs were negatively shifted with increasing alkyl chain length.[38-42] In addition, it was found that reductive desorption peaks for COOH-terminated alkanethiol SAMs on Au electrodes appeared at less negative potential compared to the corresponding CH_3-terminated alkanethiol SAMs,[42] and fluorinated aromatic thiol SAMs on Ag electrodes showed similar reductive desorption behavior to the corresponding hydrogenated aromatic thiol SAMs.[43] These results imply that the reductive desorption for organic thiol SAMs on metal electrodes occurs more easily when the organic thiols contain electron withdrawing groups, since such groups act as good electron acceptors in the reduction process. From this study, we found that the reductive desorption potential for BT SAMs with the aromatic phenyl rings was observed at a less negative potential of –566 mV, compared to alicyclic CHT SAMs (–779 mV) or CPT SAMs (–775 mV). This reductive desorption behavior for BT SAMs is due to the presence of *p*-orbitals on the phenyl rings of BTs allowing electron transfer from the Au electrode to BTs to occur more easily compared to CHT and CPT SAMs (alicyclic rings of CHT and CPT have only sp^3 hybridization). In addition, it is likely that the peak broadening for BT SAMs is related to the mixed phase with complicated adsorption configurations, as discussed above.

On the other hand, the observed peak potentials for CHT and CPT SAMs were quite similar to those of ethanethiol SAMs at around –750 mV,[42] which suggests that van der Waals interactions between alicyclic rings in CHT and CPT SAMs are nearly the same as the interactions between ethyl groups. We observed that, although the surface structures of these SAMs differed considerably (CHT SAMs have 2D ordered phase, while CPT SAMs have only a disordered phase, as shown in Figure 2(b) and 2(c)), the difference in reductive potential between CHT and CPT SAMs was quite small, implying that the magnitude of the van der Waals interactions between CHT and CPT SAMs was nearly the same. We also confirmed that the reductive desorption behavior for simple alicyclic thiol SAMs such as CHT and CPT SAMs on the Au electrode was not significantly influenced by the degree of structural order.

Conclusions

Surface structure and electrochemical behavior of self-assembled monolayers (SAMs) prepared from BT, CHT, and CPT on Au(111) surface were investigated by STM and CV. STM imaging revealed that BT and CPT SAMs on Au(111) surface contained mainly disordered domains, whereas CHT SAMs contained well-ordered domains with three domain orientations and boundaries. From this STM result, we suggest that molecule-substrate interaction is a key parameter for determining the structural order and disorder of simple aromatic and alicyclic thiol SAMs on Au(111). Moreover, we found that BT SAMs had a less negative reductive desorption peak potential of –566 mV compared to CHT SAMs (–779 mV) or CPT SAMs (–775 mV). This reductive desorption behavior for BT SAMs is due to the presence of phenyl ring *p*-orbitals, resulting in electron transfer from the Au electrode to BTs during the reduction process occurring more easily compared to CHTs and CPTs. We also confirmed that the reductive desorption behavior for simple alicyclic thiol SAMs such as CHT and CPT SAMs on Au electrodes was not significantly dependent on the degree of structural order.

Acknowledgments. This research was supported by the Basic Science Research Program through the National Research Foundation (NRF) of Korea funded by the Ministry of Education, Science, and Technology (Nos. 2010-0021448 and 2012R1A6A1029029).

References

1. Love, J. C.; Estroff, L. A.; Kriebel, J. K.; Nuzo, R. G.; Whitesides, G. M. *Chem. Rev.* **2005**, *105*, 1103.
2. Schreiber, F. *J. Phys.: Condens. Matter* **2004**, *16*, R881.
3. Vericat, C.; Vela, M. E.; Benitez, G.; Carro, P.; Salvarezza, P. *Chem. Soc. Rev.* **2010**, *39*, 1805.
4. Yang, G.; Liu, G.-y. *J. Phys. Chem. B* **2003**, *107*, 8746.
5. Krämer, S.; Fuierer, R. G.; Gorman, C. B. *Chem. Rev.* **2003**, *103*, 4367.
6. Chesneau, F.; Zhao, J.; Shen, C.; Buck, M.; Zharnikov, M. *J. Phys. Chem. C* **2010**, *114*, 7112.

7. Noh, J.; Hara, M. *Langmuir* **2002**, *18*, 1953.
8. Noh, J.; Kato, H. S.; Kawai, M.; Hara, M. *J. Phys. Chem. B* **2006**, *110*, 2793.
9. Poirier, G. E. *Langmuir* **1999**, *15*, 1167.
10. Hayashi, T.; Wakamatsu, K.; Ito, E.; Hara, M. *J. Phys. Chem. C* **2009**, *113*, 18795.
11. Ito, E.; Ito, H.; Kang, H.; Hayashi, T.; Hara, M.; Noh, J. *J. Phys. Chem. C* **2012**, *116*, 17586.
12. Ramin, L.; Jabbarzadeh, A. *Langmuir* **2011**, *27*, 9748.
13. Mamun, A. H. A.; Hahn, J. R. *J. Phys. Chem*. C **2012**, *116*, 22441.
14. Lee, N.-S.; Kim, D.; Kang, H.; Park, D. K.; Han, S. H.; Noh, J. *J. Phys. Chem. C* **2011**, *115*, 5868.
15. Wang, Y.; Chi, Q.; Hush, N. S.; Reimers, J. R.; Zhang, J.; Ulstrup, J. *J. Phys. Chem. C* **2011**, *115*, 10630.
16. Zehner, R. W. ; Parsons, B. F.; Hsung, R. P.; Sita, L. R. *Langmuir* **1999**, *15*, 1121.
17. Ramachandran, G. K.; Hopson, T. J.; Rawlett, A. M.; Nagahara, L. A.; Primak, A.; Lindsay, S. M. *Science* **2003**, *300*, 1413.
18. Virkar, A.; Mannsfeld, S.; Oh, J. H.; Toney, M. F.; Tan, Y. H.; Liu, G.-Y.; Scott, C. S.; Miller, R.; Bao, Z. *Adv. Funct. Mater*. **2009**, *19*, 1962.
19. Asadi, K.; Wu, Y.; Gholamrezaie, F.; Rudolf, P.; Bolm, P. W. M. *Adv. Mater*. **2009**, *21*, 1.
20. Lim, J. A.; Lee, H. S.; Lee, W. H.; Cho, K. *Adv. Funct. Mater*. **2009**, *19*, 1515.
21. Korolkov, V. V.; Allen, S.; Roberts, C. J.; Tendler, S. J. B. *J. Phys. Chem. C* **2011**, *115*, 14899.
22. Matel, D. G.; Muzik, A.; Gölzhäuser, A.; Turchanin, A. *Langmuir* **2012**, *28*, 13905.
23. Kang, H.; Lee, N.-S.; Ito, E.; Hara, M.; Noh, J. *Langmuir* **2010,** *26*, 2983.
24. Kang, H.; Shin, D. G.; Han, J. W.; Ito, E.; Hara, M.; Noh, J. *J. Nanosci. Nanotech.* **2012**, *12*, 557.
25. Dhirani, A. A.; Zehner, R. W.; Hsung, R. P.; Guyot-Sionnest, P.; Sita, L. R. *J. Am. Chem. Soc.* **1996**, *118*, 3319.
26. Tao, Y.-T.; Wu, C.-C.; Eu, J.-Y.; Lin, W.-L. *Langmuir* **1997**, *13*, 4018.
27. Kang, H.; Lee, H.; Kang, Y.; Hara, M.; Noh, J. *Chem. Commun.* **2008**, 5197.
28. Park, T.; Kang, H.; Ito, E.; Hara, M.; Noh, J. *Bull. Korean Chem. Soc*. **2012**, *33*, 2479.
29. Noh, J.; Hara, M. *Langmuir* **2002**, *18*, 9111.
30. Joo, S.-W.; Chung, H.; Kim, K.; Noh, J. *Surf. Sci.* **2007**, *601*, 3196.
31. Luo, P.; Bemelmans, N. L.; Pearl, T. P. *J. Phys. Chem. C* **2011**, *115*, 17118.
32. Kang, H.; Kim, Y.; Park, T.; Park, J. B.; Ito, E.; Hara, M.; Noh, J. *Bull. Korean Chem. Soc*. **2011**, *32*, 1253.
33. Waske, P. A.; Meyerbröker, N.; Eck, W.; Zharnikov, M. *J. Phys. Chem. C* **2012**, *116*, 13559.
34. Ito, E.; Noh, J.; Hara, M. *Chem. Phys. Lett*. **2008**, *462*, 209.
35. Noh, J.; Ito, E.; Hara, M. *J. Colloid Interface Sci*. **2010**, *342*, 513.
36. Stettner, J.; Winkler, A. *Langmuir* **2010**, *26*, 9659.
37. Stettner, J.; Frank, P.; Griesser, T.; Trimmel, G.; Schennach, R.; Gilli, E.; Winkler, A. *Langmuir* **2009**, *25*, 1427.
38. Qu, D.; Kim, B.-C.; Lee, C.-W. J.; Ito, M.; Noguchi, H.; Uosaki, K. *J. Phys. Chem. C* **2010**, *114*, 497.
39. Widrig, C. A.; Chung, C.; Porter, M. D. *J. Electroanal. Chem*. **1991**, *310*, 335.
40. Wano, H.; Uosaki, K. *Langmuir* **2001**, *17*, 8224.
41. Qu, D.; Kim, B.-C.; Lee, C.-W. J.; Uosaki, K. *Bull. Korean Chem. Soc*. **2009**, *30*, 2549.
42. Imabayashi, S.-I.; Iida, M.; Hobara, D.; Feng, Z. Q.; Niki, K.; Kakiuchi, T. *J. Electroanal. Chem.* **1997**, *428*, 33.
43. Schalnat, M. C.; Pemberton, J. E. *Langmuir* **2010**, *26*, 11862.
44. Scott, D. L.; Crowder, G. A. *J. Chem. Phys.* **1967**, *46*, 1054.
45. Kang, H.; Jang, C.-H.; Hara, M.; Noh, J. *J. Nanosci. Nanotech.* **2009**, *9*, 7085.
46. Käfer, D.; Bashir, A.; Witte, G. *J. Phys. Chem. C* **2007**, *111*, 10546.
47. Noh, J. *Bull. Korean Chem. Soc*. **2006**, *27*, 944.